Thermal Science and Engineering Progress 69 (2026) 104186

Contents lists available at ScienceDirect

Thermal Science and Engineering Progress

journal homepage: www.elsevier.com/locate/tsep

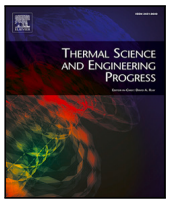

Retrofitting a CSP plant for water savings: A real case study of combined cooling at Villena-Enerstar parabolic trough power plant (Spain)

M. Lucas [a],*, J. Catalán [b]

[a] Instituto de Investigación en Ingeniería de Elche, Universidad Miguel Hernández, Avda. de la Universidad, s/n, 03202 Elche, Spain
[b] CSP Enerstar Villena Plant Director, Autovía A-31, Salida Km 175 Dirección Fontanars, 03400 Villena, Spain

ARTICLE INFO

Keywords:
Cooling tower
Air-cooled condenser
Retrofitting
Water savings
Concentrated solar power (CSP)
Combined cooling systems

ABSTRACT

This article presents a techno-economic framework for retrofitting operational Concentrated Solar Power (CSP) plants, addressing the critical challenge of water conservation in arid regions. Focusing on the Enerstar-Villena 50 MWe parabolic trough facility in Spain, this study is the first to assess combined cooling systems as a mid-lifespan upgrade, using a performance model rigorously validated against a full year of real hourly data. The validation yielded a high degree of accuracy, with a mean absolute percentage error of 1.06% for electricity generation and 0.38% for water consumption. While the model proved effective, this work also identifies key limitations within the System Advisor Model (SAM) for advanced retrofitting analyses. Five cooling configurations were assessed: the existing wet cooling towers, a fully dry air-cooled condenser, and three parallel combined setups. The analysis demonstrates that the air-cooled condenser achieved the greatest water savings (91.5%) but reduced net energy output by 11.5%. In contrast, combined systems offer an optimal solution, maintaining energy production within 1% of the wet-cooled baseline while reducing water use by 24%–69%. The 50% wet–dry configuration provides the best technical and economic balance, preserving energy output while cutting water consumption by nearly half. An economic assessment indicates this system achieves a payback time as short as 6.14 years, confirming its viability as a strategic enhancement for aging CSP assets

1. Introduction

The transition of the energy system towards renewable sources is essential for effectively addressing climate change. According to projections by the International Energy Agency (IEA) in its Net Zero Emissions by 2050 scenario, the global share of renewable energy generation is expected to increase significantly, rising from approximately 28% in 2021 to 88% by 2050, [1]. While photovoltaic (PV) and wind energy are the most mature technologies significantly contributing to the global decarbonization of electricity systems, both share a fundamental limiting factor: their production is inherently dependent on the variability of meteorological phenomena. This necessitates balancing supply and demand through various strategies, such as developing energy storage solutions, adapting consumption patterns to production, or advancing renewable technologies with flexible generation capabilities, [2]. Concentrated Solar Power (CSP), unlike other renewable energy sources, has the capability to adjust electricity production according to the needs of the power system due to its ability to incorporate thermal energy storage. This technology has demonstrated its potential for large-scale electricity generation, with 7 GW installed worldwide in 2021 and significant projected growth, reaching an estimated 437 GW by 2050, [1].

The design of concentrated solar power (CSP) plants has been diverse in terms of concentration systems (including Stirling dishes, to a lesser extent, linear Fresnel reflectors, solar power towers and parabolic trough collectors), as well as in the choice of heat transfer fluids, power block configurations, and the inclusion or exclusion of thermal storage. This diversity means that the maturity and optimization of CSP plant designs are still evolving. Addressing challenges such as reducing installation and operational costs while minimizing environmental impact is essential to enhancing the competitiveness of these plants, making the current stage particularly exciting from an engineering perspective. One of the critical design decisions in CSP plants is the selection of the condensation system to be employed, [3].

The thermal performance of a CSP plant is largely determined by the pressure and temperature of the steam entering and exiting the turbine. In turn, the pressure and temperature at the turbine outlet are limited by the condensation medium. The lowest ambient temperature that can be achieved with conventional condensation systems is the wet-bulb

* Corresponding author.
E-mail address: mlucas@umh.es (M. Lucas).

https://doi.org/10.1016/j.tsep.2025.104186
Received 9 September 2025; Received in revised form 29 September 2025; Accepted 6 October 2025
Available online 28 October 2025

Nomenclature

A	Total heat transfer area of the condenser (m^2)
C_C	Cycles of Concentration [–]
c_p	Specific heat capacity of water (J kg^{-1} K^{-1})
f_{drift}	Drift fraction [–]
f_{wc}	Wet cooling fraction [–]
$\dot{m}$	Mass flow rate (kg s^{-1})
P_c	Hybrid system condenser pressure (Pa)
$P_{c,ACC}$	Condenser pressure from ACC-only operation (Pa)
$P_{c,WC}$	Condenser pressure from wet cooling-only operation (Pa)
P_{cycle}	Net electrical power output of the cycle (W)
$\dot{Q}_{rej}$	Total heat rejection rate (W)
$\dot{Q}_{rej,dry}$	Heat rejection rate from the dry system (ACC) (W)
$Q_{rej,wet}$	Heat rejection rate from the wet cooling system (W)
T_{cond}	Condenser saturation temperature (K)
$T_{cw,in}$	Cooling water inlet temperature (K)
$T_{cw,out}$	Cooling water outlet temperature (K)
T_{db}	Ambient dry-bulb temperature (K)
T_{wb}	Ambient wet-bulb temperature (K)
U	Overall heat transfer coefficient (W m^{-2} K^{-1})

Greek symbols

η_T	Power cycle thermal efficiency [–]
Δh_{evap}	Latent heat of vaporization of water (J kg^{-1})
ΔT_{app}	Cooling tower approach temperature (K)
ΔT_{cw}	Cooling tower range (K)
ΔT_{out}	Condenser terminal temperature difference (TTD) (K)

Subscripts

bd	Blowdown
cw	Circulating water
drift	Drift losses
evap	Evaporation
makeup	Makeup water
a	Air
s	Saturated
v	Vapor
w	Water

Abbreviations

ACC	Air-Cooled Condenser
AP	Adiabatic Pre-cooling
CSP	Concentrated Solar Power
HTF	Heat Transfer Fluid
IEA	International Energy Agency
ITD	Initial Temperature Difference
LCOE	Levelized Cost of Electricity
MAPE	Mean Absolute Percentage Error
NREL	National Renewable Energy Laboratory
PC	Power Cycle
PSA	Plataforma Solar de Almería
PV	Photovoltaic
RMSE	Root Mean Squared Error
SAM	System Advisor Model
SCA	Solar Concentrator Assembly
SCE	Solar Collector Element

temperature. This is why most CSP plants use cooling towers, which operate based on the evaporative cooling of the water stream coming from the condenser. The effect of modifying the condensation temperature on the power output of the plant is approximately 0.5% to 1% per degree Celsius, according to [4]. Although cooling towers achieve a lower condensation temperature and, therefore, better thermal performance, there are several drawbacks that must be considered during the design phase of these plants. The main issue relates to the water consumption associated with these systems, ranging from approximately 2.3 to 3.4 m^3/h per MWe, according to [5]. It is important to highlight that the geographic areas where CSP plants are most productive — those with high levels of direct irradiation — are often regions with severe water scarcity.

One strategy proposed to drastically reduce water use in condensation is the implementation of air-cooled condensers. It is estimated that by using air-cooled condensers, water consumption in CSP plants can be reduced by 80%–90%. In this case, the plant's water use is limited to purposes other than cooling, such as cleaning parabolic trough collectors, replenishing water in the power block, and other less significant uses. Another advantage of using dry cooling systems is the elimination of the visible plume produced at the cooling tower outlet during cold periods, which occurs when the humid exhaust air mixes with the ambient air. This is particularly relevant for CSP plants, as the presence of the plume can reduce the efficiency of collectors located near the cooling tower. However, despite the significant potential for water savings with dry cooling systems, they have certain drawbacks. These include a reduction in power generation, an increase in auxiliary power demand (since air-cooled condensers require higher electricity consumption for ventilation compared to wet systems), and higher capital costs. Among the pioneers in the comparative study of water versus air condensation are [6,7], and [8]. They confirmed that the significant reduction in water consumption offered by dry cooling systems comes with a penalty in the plant's overall performance and power output.

The growing interest in hybrid or combined heat dissipation systems is challenged by a fundamental inconsistency in the associated terminology. The ambiguous use of terms such as 'hybrid', 'combined', 'evaporative', and 'adiabatic' leads to a lack of clarity in the classification of these refrigeration systems. In this article, the term 'Combined System' will be used to describe a system that simultaneously employs two traditional, independent cooling units (one dry and the other incorporating evaporative cooling), connected either in series or in parallel, in line with the terminology proposed by [9]. Additionally, the term ''Hybrid System'' will be reserved for technologies that integrate within a single unit evaporative cooling mechanisms and also include a coil capable of operating exclusively in dry mode under specific environmental conditions. The market offers a wide variety of innovative configurations, which can be broadly classified into those designed for plume abatement and those aimed at reducing water consumption. The first study introducing a hybrid cooling system for a CSP power cycle was conducted by [10], comparing wet, dry, and hybrid condensation systems with air pre-cooling via an adiabatic pad. Using the Andasol I plant (50 MWe, Granada, Spain) as a reference, they performed energy, exergy, and environmental analyses. Results showed that the wet system achieved the lowest condensation pressure and highest efficiency, with a 12.60% gain over the dry system. The hybrid system

improved efficiency by 4.65% compared to the dry case, while reducing water consumption by 71.74% relative to the wet system, with only a 7.06% drop in net power. Thus, the hybrid configuration was identified as a promising compromise between water savings and performance.

Following Cutillas, [11] examined a hybrid system using spray adiabatic pre-cooling (AP), combining simulations and experiments. They evaluated CSP efficiency, water use, output, and costs against dry and wet cooling. Results showed that efficiency gains were minor beyond 80% saturation, but at 99% AP improved efficiency by 1.61% over dry cooling while reducing water use by 14.61% compared to wet cooling. A 10-point increase in saturation raised water use by 26.75%, cut parasitic energy by 5.37%, and increased capacity factor by 0.35%. Overall, AP was identified as a promising option to balance efficiency and water savings in CSP plants. [12] proposed a combined system that involves the simultaneous parallel installation of a cooling tower and a dry heat exchanger, selecting one system or the other depending on environmental conditions. This approach achieved water savings of over 70% while minimally impacting plant production, with only a 3% reduction. [13] presented a comprehensive environmental assessment of combined cooling systems in central tower Concentrated Solar Power (CSP) plants. Using Life Cycle Assessment (LCA) methodology, the research analyzed two optimized configurations based on the recently constructed Redstone CSP plant in South Africa. [14], studied the integration of a combined cooling system into a 50 MWe power block (with the same configuration as the CSP plant Andasol-1) using the Thermoflex simulation tool to evaluate its performance under different configurations. They showed that a significant reduction in water consumption was possible with minimal impact on power generation. In a series–parallel combined system with a wet cooling tower at 50% capacity, water use decreased by 40%, while power generation dropped by only 0.7% compared to a full-capacity system. The series–parallel configuration achieved the highest water savings (up to 62%) compared to wet cooling alone, while the parallel configuration maximized power output, increasing generation by 3.2% while reducing water use by 30%. These results highlight the potential of combined cooling systems to enhance CSP plant efficiency and sustainability. Building on a similar approach but with more versatile hydraulic configurations, [15] reported experimental results from their pilot plant at the Plataforma Solar de Almería (PSA). They tested serial and parallel setups under different conditions, showing high potential for water savings compared to a fully wet system. In particular, a 25% wet/75% dry parallel connection achieved 67% water savings, while the 50/50 configuration reduced fan power by 59% relative to the dry system. Using two efficiency indices — specific electricity and water consumption — the parallel configuration was found optimal in most cases, especially at high temperatures and 80% load. While the work carried out at the PSA experimental plant is highly noteworthy, there are still areas for further research, such as understanding the influence of relative humidity and refining the efficiency indices.

The literature reviewed includes comparative studies on condensation systems for CSP plants, encompassing both hybrid or combined system, all with a decision-making perspective during the plant design phase. We are now entering a phase where the retrofitting of spanish CSP plants, built at the end of the first decade of this century, and now reaching the midpoint of their operational lifespan, is becoming a key consideration. This temporal context defines the present study, providing a different perspective compared to previous research. The optimization of the heat dissipation system is a strategic priority for plant operators in anticipation of potential future water consumption restrictions due to drought periods, which could force shutdowns compared to other renewable technologies. Furthermore, in a less extreme scenario, such optimization can enhance the plant's operational flexibility, allowing for improved water consumption management and energy production optimization based on time-of-delivery tariff structures.

The originality of this paper is based on three fundamental pillars. First, to the best of the authors' knowledge, hybrid or combined cooling systems have not yet been implemented in the power cycle of commercial concentrating solar power (CSP) plants. Second, the existing scientific literature on the subject is limited to comparative studies of condensation systems, including hybrid or combined technologies, but invariably from a decision-making perspective during the design phase of new plants. In contrast, this study introduces a novel techno-economic analysis focused on the retrofitting of an existing cooling system. Finally, the third contribution of this work lies in the validation of a model based on the System Advisor Model (SAM) software at an hourly resolution, in terms of both energy generation and water consumption, a methodological approach that has not been previously reported in the literature.

This research primarily aims to assess the optimal configuration of a combined cooling system for a potential retrofit of the Enerstar-Villena CSP plant (Spain). The central focus is on maximizing power generation while minimizing water consumption. A predictive model, developed using SAM software, is employed to characterize the performance of the CSP plant. In addition to its primary objective, this study significantly contributes to the field by validating the model's accuracy in predicting power production and water consumption using a complete year (2024) of real operational data from the Enerstar-Villena plant, thereby filling a critical void in the current published literature concerning the real-world application of such models. A secondary but no less important objective is to understand the capabilities and limitations of SAM in these types of comparative retrofitting studies. Ultimately, the analysis of the trade-offs between energy production and water savings serves to inform the techno-economic viability of implementing such retrofits to improve the plant's long-term sustainability and performance.

The paper is structured as follows: Section 2 details the methodology, including the description of the plant and the development and validation of the performance model using SAM software and real operational data from 2024. Section 3 presents the key equations used in the modeling of the cooling systems studied and the key issues for their comparison. Section 4.1 compares the different heat dissipation strategies in terms of power produced and water consumption. Finally, Section 5 summarizes the key findings, highlighting the techno-economic viability of the proposed retrofits, and provides recommendations for future research.

2. Method

2.1. Enerstar-Villena CSP power plant description

Enerstar-Villena CSP Plant is a 50 MWe parabolic trough (CCP) solar thermal power plant without thermal energy storage. Located in Villena (Alicante), Spain, the latitude and longitude location is 38.72° North −0.92° West. The solar field, with a total aperture area of 339,506 m^2, is divided into five subfields and comprises 105 loops, see Fig. 1, each containing four 150 m long Solar Concentrator Assemblies (SCAs) for a total of 420 SCAs. Each of the SCAs is controlled by a hydraulic group. By adjusting their orientation, the temperature of the thermal fluid can be regulated. Within the Villena solar field, SCA configurations can be found in either a U-shaped or W-shaped arrangement. The range of motion of an SCA ranges from −20° to 200°. However, the effective operating range is between 10° and 170° due to shading from adjacent rows. The stow position is set at −10° relative to the horizontal. Each solar collector (SCA) is composed of 12 Solar Collector Elements (SCE), featuring SenerTrough (SNT-1) collectors from Sener (Spain). Finally, each SCE is composed of 3 heat collection elements (HCE) consisting of 28 mirrors, RP3 Flabeg (Germany), and receivers, model Schott PTR®70, designed for use in state-of-the-art power plants operating with oil-based heat transfer fluids (HTF) at temperatures up to 400 °C. The plant utilizes the parabolic trough collectors to heat Dowtherm A heat transfer fluid to between 293 °C and 393 °C. This is a eutectic mixture of two highly stable compounds: biphenyl ($C_{12}H_{10}$) and diphenyl oxide ($C_{12}H_{10}O$). These compounds have nearly identical

Fig. 1. Distribution of the solar subfields of the Ernestar-Villena plant (Dark blue). Power block (White). (For interpretation of the references to color in this figure legend, the reader is referred to the web version of this article.)

vapor pressures, allowing the mixture to be handled as if it were a single compound. The atmospheric boiling point of HTF is 257.1 °C and the freezing point is 12 °C. However, for operational safety reasons, a higher service temperature limit of 65 °C is established. The approximate total inventory of HTF in the system is 1350 tons. The heated HTF drives a steam Rankine cycle with reheat, operating at 100 bar, to power a MAN Turbo turbine. Steam condensation occurs in a shell and tube condenser cooled by recirculated water from a three-cell, counterflow, induced draft, three-cell cooling tower as a heat sink from Hamon-Esindus. As part of the contextualization of the plant's design and construction, the nominal design capacity was limited to 50 MWe to qualify for the special regime incentives established in Spanish Royal Decree 661/2007. The construction of the plant was completed in October 2013, and since February 2014, the plant has been connected to the grid and in commercial operation.

Table 1 summarizes the technical data from Enerstar-Villena CSp plant recorded in the National Renewable Energy Laboratory database [16], supplemented with additional information.

2.2. Enerstar-Villena CSP power plant SAM model. Baseline case

The System Advisor Model (SAM) is a techno-economic model maintained and developed by the National Renewable Energy Laboratory (NREL). It is a widely used tool for predicting the annual performance and financial viability of concentrated solar power (CSP) systems. It has a flexible interface, allowing users to incorporate their own external performance models into the SAM framework for sensitivity analysis, annual performance predictions, or financial modeling. SAM includes performance models for different CSP technologies, such as parabolic trough collectors, power towers, and Dish–Stirling systems. SAM's performance models use system geometry data, optical properties, weather data, and fluid thermodynamic properties to calculate component performance. Model formulations generally use first-principle or semi-empirical approaches and, consequently, account for a wide range of potential performance effects. Fig. 2, illustrates a schematic of the information flows employed in the model construction and validation process. In the initial stage, the technical specifications of the plant are input into the SAM model, along with the environmental variables measured throughout 2024.

Based on imported weather data, the software facilitates its analysis and processing, offering annual metrics and graphical representations, including monthly, daily, and hourly temporal evolutions, frequency histograms, and heat maps. Fig. 3 shows, as an example, the evolution in hourly resolution of environmental variables throughout the year. The program also facilitates the visualization of month-by-month hourly profiles, exemplified in Fig. 4 by the illustration of the beam, diffuse, and global irradiance components of solar radiation.

Following the input of weather data and technical specifications into the model, the simulation is executed. The summary of the plant's annual operational data is presented in Fig. 5, where key annual results include over 94,694 GWh-e of gross electricity produced; 79,088 GWh-e injected into the grid, resulting in a capacity factor of 18.1%; and a water consumption of 277,443 m^3. SAM provides a wide array of options for generating tables and graphs from the simulation outputs, which are omitted here for brevity.

Beyond its integrated graphical capabilities, SAM allows for the export of data at the aforementioned frequencies for subsequent processing in external software. Using the exported data, a detailed analysis and breakdown of the results can be performed, particularly concerning the power output: gross, net, and grid-injected power. The subsequent Sankey diagram, which illustrates these energy flows, was generated from SAM-exported information using dedicated software, [17] (see Fig. 6).

The discrepancy between Power Cycle (PC) electrical power output Gross and Total electric power to grid (also referred to as Net Power in earlier SAM versions) arises from parasitic electrical consumption within the solar field and power block, encompassing pumps, cooling equipment, and other auxiliary loads. The "Total electric to the grid" represents the power output of the power cycle prior to the application of "System availability losses" losses. By default, a 4% system availability loss is applied, accounting for the difference between the aforementioned variables.

Furthermore, it is important to note that the variable "Total electric to the grid" is positive during plant operation but can be negative at other times due to fixed parasitic loads. Consequently, for the subsequent validation analysis, a distinction is made between: Total electric to the grid 82,383 MWh = (Net > 0 Electric Output (MWh); 88,453 MWh) + (Net < 0 Electric Output (MWh), Hourly; −6070 MWh).

2.3. SAM model validation

Validating the System Advisor Model (SAM) is essential for ensuring the reliability of simulations used in the design and retrofitting of concentrating solar power (CSP) plants. This process, involving the comparison of model outputs with real-world data, is vital for correcting systematic errors, improving accuracy, and optimizing facility performance under specific environmental conditions.

Table 1
Enerstar-Villena CSP plant specifications.

Location	Villena (Spain)
Break ground date	2010
Expected generation (GWh/year)	100
Lat/Long location	38.729, −0.922
Total power station land area (km^2)	2.1
Developer	FCC Energy, Spain
EPC	FCC, IDOM, Spain
Plant configuration — Solar field	
Solar field aperture area (m^2)	339 506
# of Solar Collector Assemblies (SCAs)	420
# of Loops	105
# of SCAs per Loop	4
# of Modules per SCA	12
SCA Length (m)	150
Collector/Heliostat manufacturer	Sener, Spain
Collector/Heliostat engineering or IP owner	Sener, Spain
Collector/Heliostat model	SenerTrough
Mirror manufacturer	Flabeg, Germany
Mirror model	RP3
Solar field (Receiver)	
Receiver working fluid	Dowtherm A
Receiver working fluid category	Thermal oil/organics
Solar field or receiver inlet temperature (°C)	293
Solar field or receiver outlet temperature (°C)	393
Receiver manufacturer	Schott, Germany
Receiver model	PTR 70
Power block	
Nominal turbine or power cycle capacity	50 MW
Turbine manufacturer	MAN Turbo, Germany
Power cycle	Steam Rankine
Power cycle pressure	100 bar
Cooling system	
Cooling type	Wet (Cooling tower)
Type of cooling tower	Counterflow, Induced Draft, 1 × 3 Cells
Circulating water flow — Total	2.230
Design heat duty	91.44 MW
Design dry bulb temperature	28.4 °C
Design relative humidity	70.0
Design wet bulb temperature	24.0
Cycles of concentration	2.9

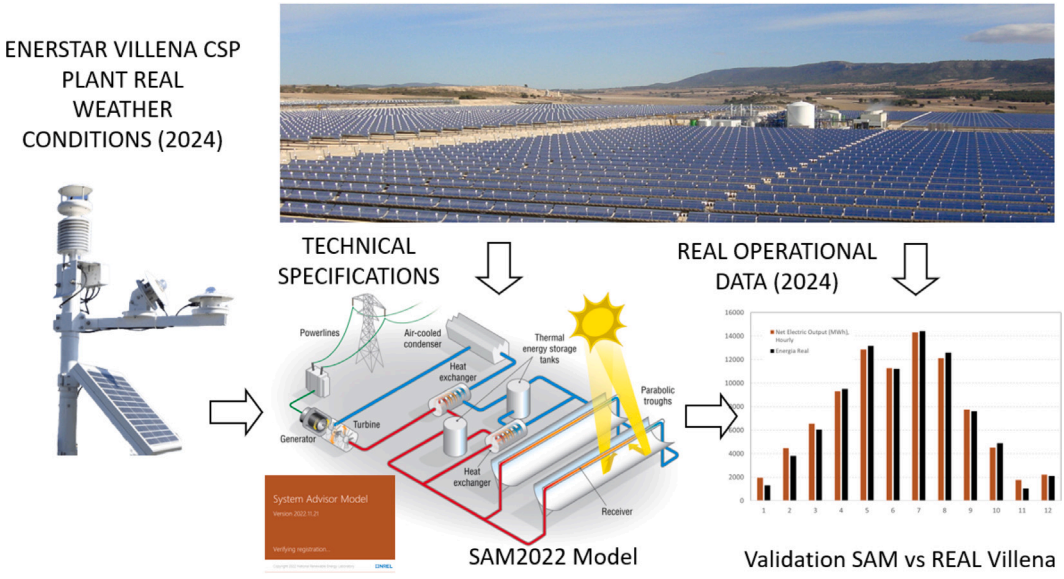

Fig. 2. Information flows for SAM2022-Based CSP plant model construction and validation.

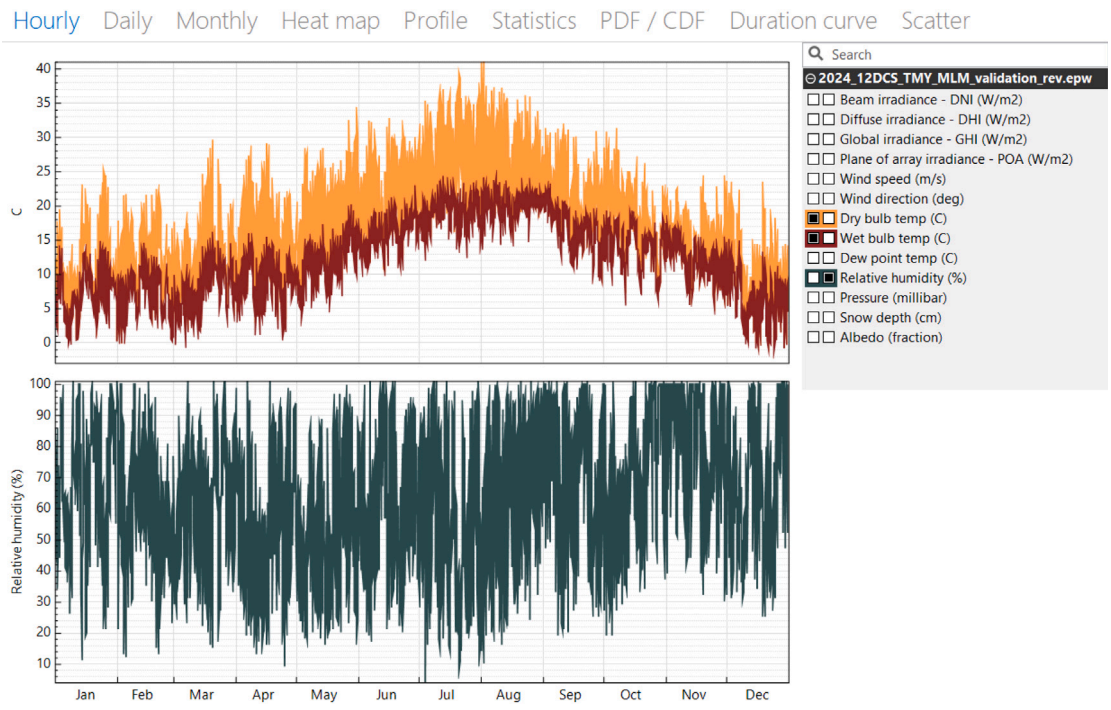

Fig. 3. Hourly evolution of dry bulb temperature, Wet bulb temperature and relative humidity throughout 2024 at the Enerstar-Villena CSP plant.

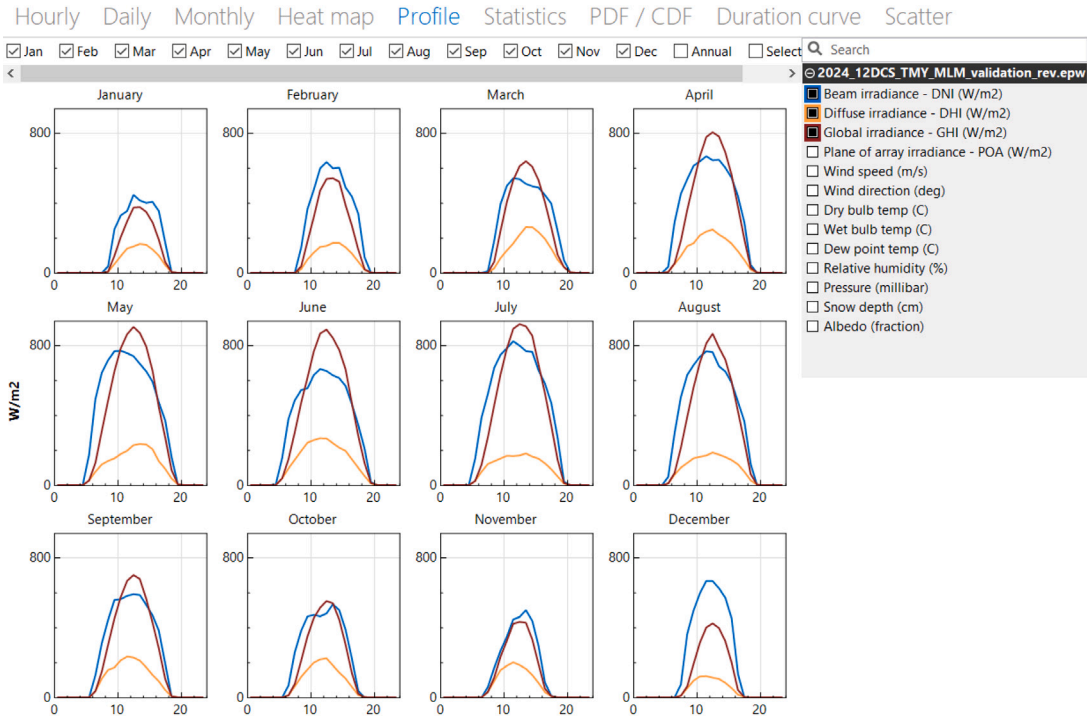

Fig. 4. Monthly hourly profiles of beam, diffuse, and global irradiance at the Enerstar-Villena CSP plant throughout 2024.

2.3.1. SAM model — Validation review

Documented validation exercises for SAM have shown significant limitations. The NREL's own documentation [18] refers to early studies of one parabolic trough (Andasol-1) and one solar tower (Gemasolar) plant. These validations are methodologically constrained, relying on comparisons of a single annual energy output figure against estimations, an approach inadequate for validating complex hourly simulations and the dynamic interactions between components. [19] took a significant step forward by proposing an improved validation exercise for SAM based on available electricity production data from the US Energy Information Administration (EIA). The validation considered both parabolic trough (Genesis, Mojave, and Solana) and solar tower (Crescent Dunes) technologies. Computed monthly average capacity factors were compared against measured operational data, showing relatively good agreement for the parabolic trough systems but a substantial deviation for the solar tower system. The authors noted that while monthly averaging smooths out discrepancies, higher-frequency data is essential for a truly rigorous validation. The study concluded

Metric	Value
Annual AC Energy in Year 1	79,088,952 kWh-e
Annual Freeze Protection	0 kWh-e
Annual TES Freeze Protection	0 kWh-e
Annual Field Freeze Protection	0 kWh-e
Capacity factor	18.1%
Power cycle gross electrical output	94,694,008 kWh-e
First year kWh/kW	1,582 -
Gross-to-net conversion	83.5 %
Annual Water Usage	277,443 m^3

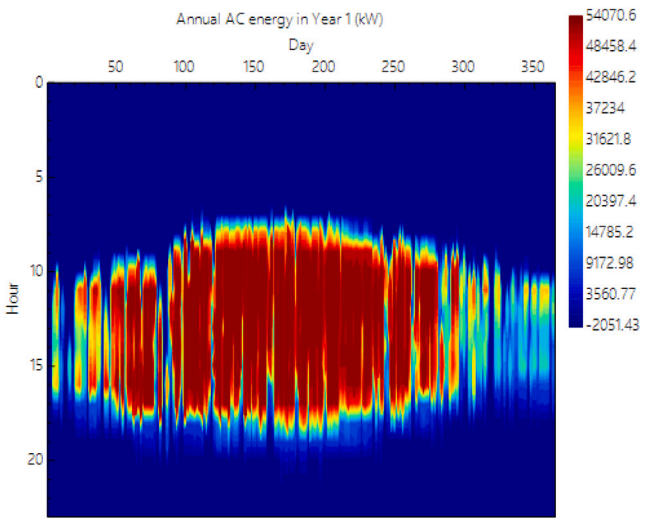

Fig. 5. Enerstar-Villena CSP plant SAM annual performance.

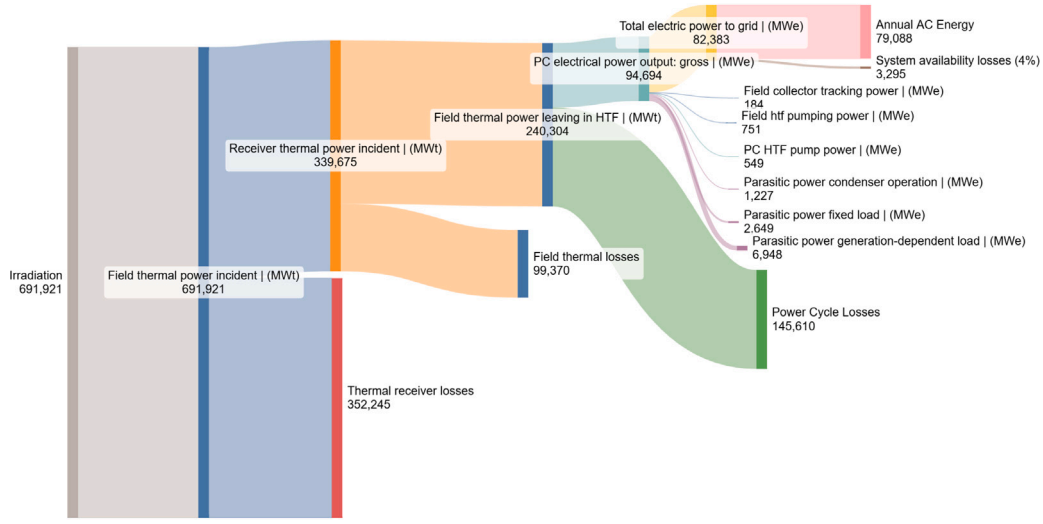

Fig. 6. Sankey diagram depicting the main energy flows in Enerstar-Villena CSP plant SAM simulation.

that without such detailed validation, SAM's hourly outputs can only be considered very rough estimations of the power cycle's performance, as they have not been compared against similarly detailed experimental data at the component or system level. Therefore, the work established the necessity of collecting high-frequency data to perform a proper validation and refine the many semi-empirical models used within SAM. Building on this, [20] validated a 140 MWe CSP plant model for two locations in Jordan using a monthly resolution, reaffirming the need for experimental data and the impact of local environmental factors. While [21] presented an hourly-resolution validation, its applicability is limited due to the plant's small scale (50 kWe), use of water as the thermal fluid, and a short validation period of only 10 days. This article addresses this research gap by presenting an hourly validation of SAM for both energy production and water consumption, using a full year of operational data from the exceptionally reliable Enerstar-Villena solar plant.

2.3.2. Enerstar-Villena CSP plant SAM model — validation. Energy

This section compares the results obtained from the SAM model with the operational data measured at the Enerstar-Villena plant during its routine commercial operation in 2024. This validation process refers to the variable that has been designated as "(Net > 0 Electric Output (MWh), Hourly)" and which reflects the energy fed into the grid, disregarding instances when this variable is negative, indicating that there are times of the day when there is no production and only consumption. This criterion is adopted following the operational guidelines of the plant. Furthermore, days on which the plant did not operate due to its own decisions, conditioned by the grid or maintenance, have not been considered in the validation. Regarding maintenance tasks, two annual mini-shutdowns were carried out (one in January and another in November) for turbine inspection, which involved 4 days encompassing turbine cool-down, maintenance actions, and the restoration of thermal start-up conditions. Specifically, the actions carried out on those days included: Review of tolerances in the Blades and the Rotor; Review of axial bearings and Shaft Alignment; and Checking of seals and Clearances in the Turbine Casing. In addition, mandatory safety pressure tests were performed on different components of the plant. Thermography was carried out to inspect welds. Furthermore, the cooling tower cleaning and disinfection processes were performed in accordance with the national regulations against Legionella, [22]. To clarify this idea, the reader is referred to Fig. 7, which shows the daily production values. Some days at the end of January and in November can be observed in which the plant could have operated based on available radiation, as recorded by SAM, but it did not. To ensure

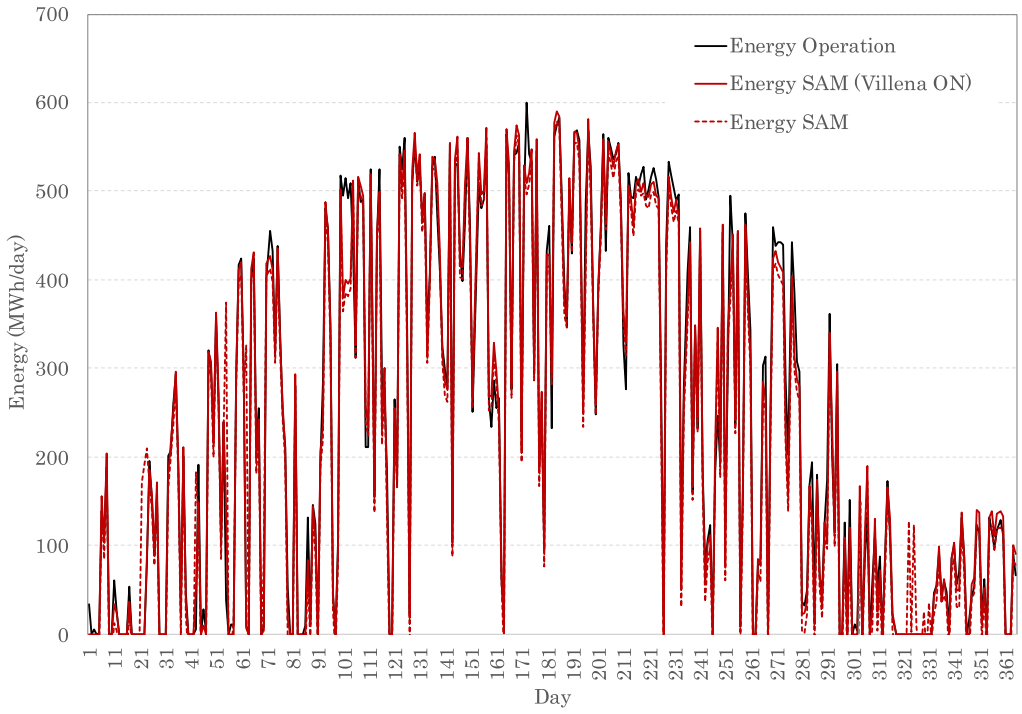

Fig. 7. Daily energy production validation: SAM vs. Real data.

the integrity of the validation dataset, periods of plant unavailability, such as scheduled maintenance and solar field cleaning, were excluded. Corresponding outliers were identified from the operational logs and removed manually, so that the validation reflects model performance under normal operating conditions.

In terms of annual production, the mean absolute percentage error (MAPE) is $MAPE_{annual}$ = 1, 06% = 1. 06%, and in terms of monthly production, the average error is $MAPE_{monthly}$ = 2.23%. Taking into account the monthly results, see Fig. 8, the largest errors occur in the winter months, particularly in January and November. These months are when the plant operates for the fewest number of days, and therefore the thermal inertia effects of all systems are more pronounced.

Fig. 9 shows a combination of monthly and daily results. For this purpose, a very common parameter used to represent the behavior of power generation plants is utilized: the Capacity Factor (CF), (Eq. (1)). This represents the energy production of a power generation plant in comparison to its maximum nominal capacity in Villena (50 MW) if it were operational at all times for a given period.

$$CF = \frac{Energy\ Production\ (\text{MWh})}{Nominal\ Power\ x\ time\ (\text{MWh})} \tag{1}$$

In quantitative terms, the calculated Root Mean Squared Errors ($RMSE$) are $RMSE_{CFmonthly}$ = 1.06% and $RMSE_{CFdaily}$ = 3.36%. It can be observed how the order of magnitude and the trends shown coincide with the graphs presented in the work of [19]. For the representation of daily behavior, a scatter plot is also used, where the ±10% error reference lines have been included. The data show that out of the 272 days the plant operated, 158 are within 10% error and 202 are within 20% error, see Fig. 10.

Moving on to an hourly resolution, Fig. 11 shows, as an example, the comparison between the model and the experimental data for the month of June, with good agreement observed between the two.

The model's performance can also be represented in terms of monthly production by hourly bands, see Fig. 12. As mentioned in the monthly data analysis, the largest discrepancies are found in the winter months. Furthermore, this data visualization also reveals a slight lag in production at the end of the day again justified by the thermal inertia of the plant's components and fluids. At an hourly resolution, out of the 2990 h that the plant is operational, 2457 h show production within the MAPE ±10% interval.

2.3.3. Enerstar-Villena CSP plant SAM model — validation. Water consumption

In addition to energy production, water consumption represents the second critical parameter in assessing the most suitable cooling system. The total water consumption in a cooling tower represents the sum of water losses through evaporation, blowdown, and drift. Evaporation is the primary loss mechanism, where water transforms into vapor and is released into the atmosphere, removing heat from the remaining water. Blowdown, or bleeding, is the controlled extraction of water to limit the concentration of dissolved solids, preventing scaling and corrosion. Drift is the loss of water droplets carried by the airflow through the tower. Makeup water must compensate for these losses to maintain the desired water level in the system. The calculation of evaporated water utilizes mass and energy balances applied to the water and air streams. These balances can be executed with precision using the equations proposed by [23], or through a simplified calculation that neglects the evaporated water in the water mass balance. SAM defaults to the simplified option based on the latent heat of vaporization of water.

$$\dot{m}_{evap} = \frac{\dot{Q}_{rej}}{\Delta h_{evap}} \tag{2}$$

Drift is typically of lesser quantitative significance and conditioned by the drift eliminator efficiency; a value of 0.001% of the circulating water in the cooling tower is considered in SAM for this term. However, its environmental and public health relevance is considerable. Drift consists of the emission of aerosolized droplets that contain dissolved solids and treatment chemicals from the circulating water, which can adversely affect local vegetation and infrastructure. Critically, these aerosols can also serve as a vector for the dispersal of waterborne pathogens, such as Legionella pneumophila, posing a significant public health risk. Therefore, compliance with the national regulatory framework for the prevention and control of Legionellosis is required, [22].

$$\dot{m}_{drift} = f_{drift}\dot{m}_{cw} \tag{3}$$

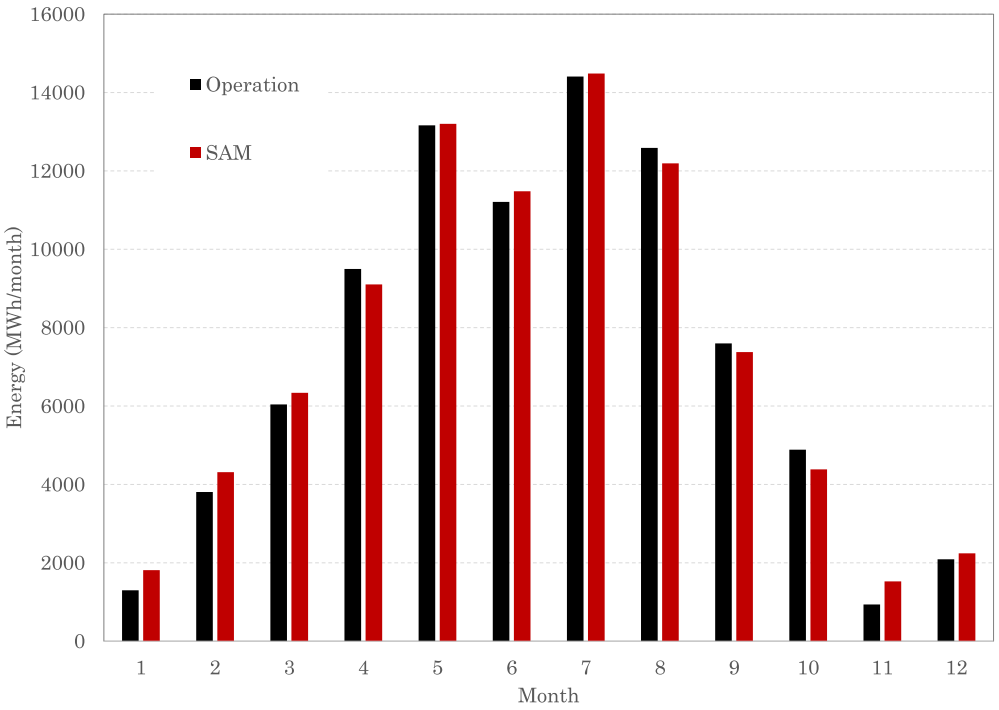

Fig. 8. Monthly energy production validation: SAM vs. Real data.

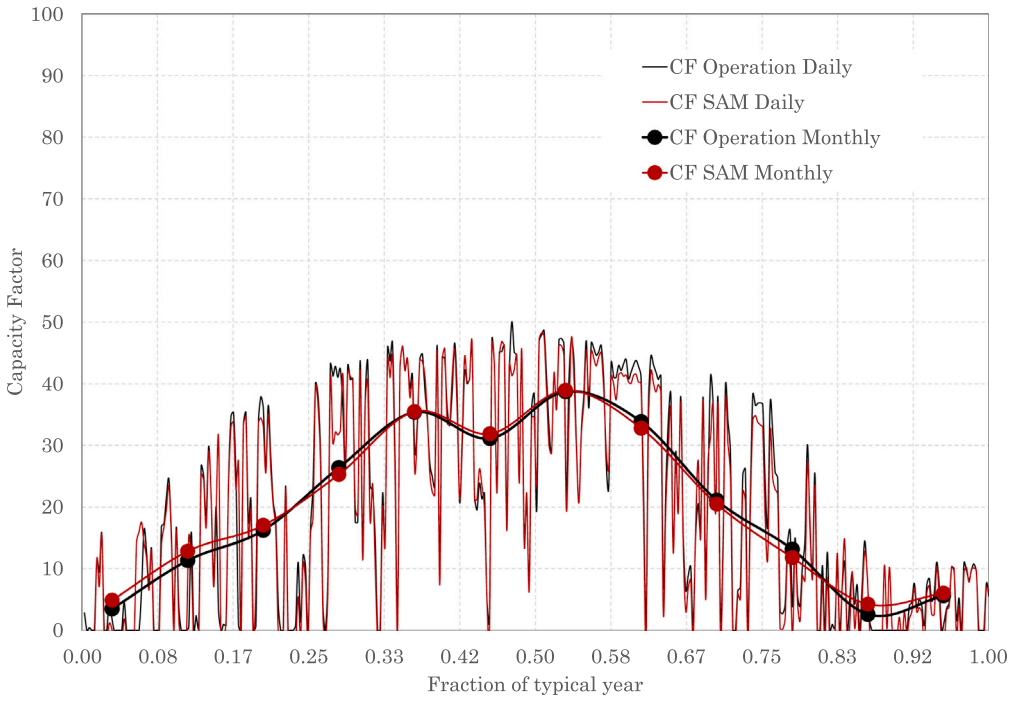

Fig. 9. Monthly and daily capacity factor: SAM vs. Real data.

For the determination of blowdown, the concept of Cycles of Concentration (C_C) is employed. This represents the ratio between the concentration of dissolved solids in the blowdown water and the dissolved solids in the makeup water, see [24]. Considering the limits imposed by the inlet water quality and legal restrictions on water discharged to the public drainage network, an annual average cycles of concentration value of 2.9 is employed.

$$\dot{m}_{bd} = \frac{\dot{m}_{evap} + \dot{m}_{drift}}{C_C - 1} \tag{4}$$

Therefore, the value of the makeup water is:

$$\dot{m}_{makeup} = \dot{m}_{evap} + \dot{m}_{drift} + \dot{m}_{bd} \tag{5}$$

At the Enerstar-Villena solar thermal plant, the recorded variables include both makeup water and blowdown water. Thus, the combined value of evaporated water and drift is calculated as the difference between these measured quantities. Following the same method used to represent energy values at different temporal scales, the same can be done for water consumption. However, for the sake of conciseness, only the most relevant graphs related to water consumption are presented.

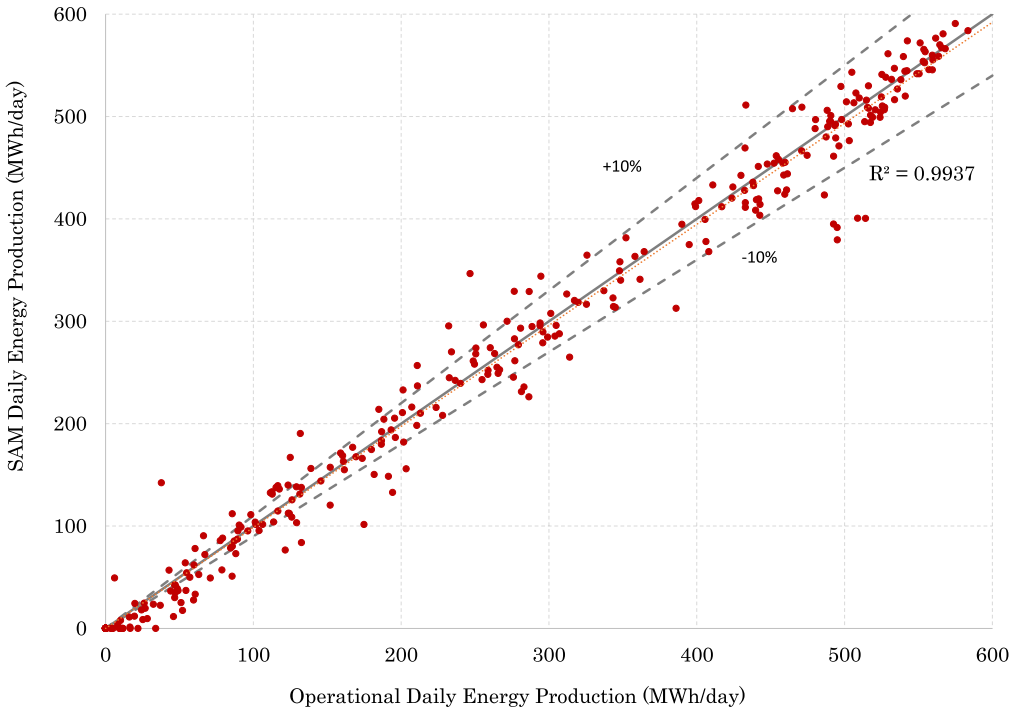

Fig. 10. SAM daily energy production vs. Real daily energy production.

Fig. 11. SAM and real power production (June).

Based on plant operational history, several clarifications regarding water consumption are noteworthy, as they directly affect the processing and subsequent analysis of these data. Two specific consumption events are identified in Fig. 13. Both are justified by maintenance actions based on cleaning and disinfection, derived from compliance with national regulations regarding the sanitary requirements for the prevention and control of legionellosis.

Furthermore, it has been found that performing a mass balance on an hourly timescale can result in physically inconsistent outcomes, such as negative evaporation rates. These anomalies arise due to the dynamic behavior of the system, particularly the role of the cooling tower basin, which introduces a temporal phase lag between the various components contributing to the overall mass balance. Specifically, blowdown events may occur during periods when the cooling tower is inactive, leading to an apparent negative evaporation rate in the computed balance. This highlights the importance of accounting for transient storage effects and system inertia when analyzing short-term mass flows in such systems.

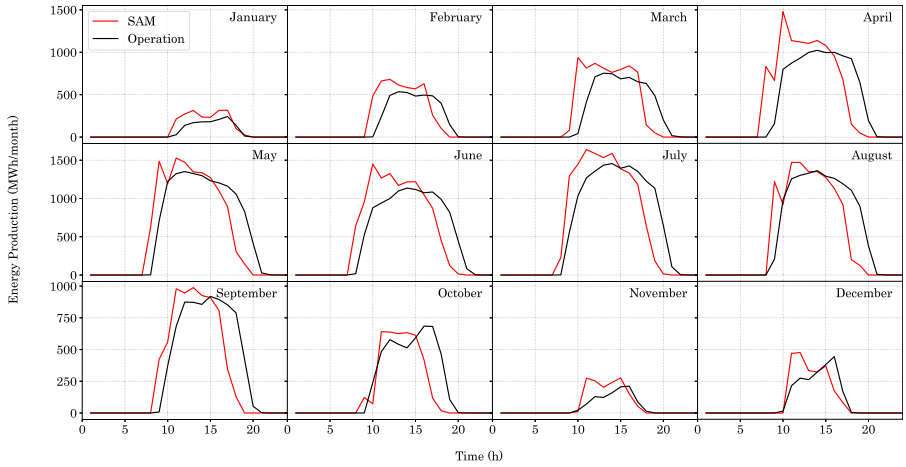

Fig. 12. Monthly energy production by hourly bands.

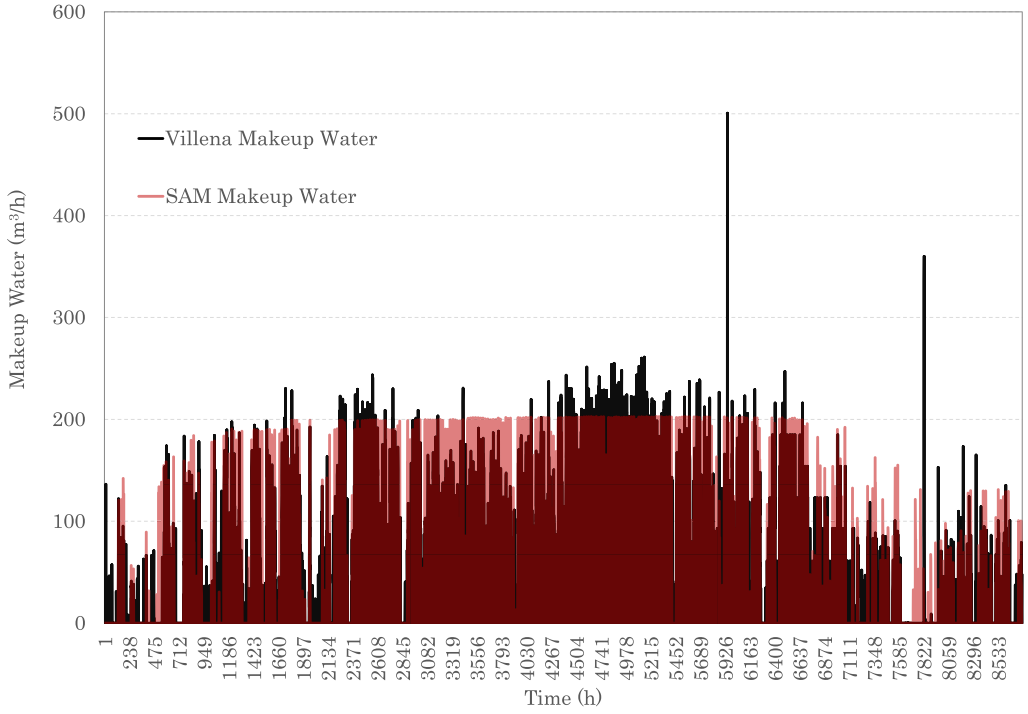

Fig. 13. SAM and real makeup water consumption. Hourly data.

This effect is no longer observed when the analysis is performed on a daily timescale, see Fig. 14.

Regarding the results generated by SAM, a tuning can be performed based on the total makeup water by modifying the blowdown term. Thus, annual errors, $MAPE_{annual(makeup)}$ = 0.38%, $MAPE_{annual(evap+drift)}$ = 15.35%, and $MAPE_{annual(blowdown)}$ = 30.22% are achieved. However, aligning the total evaporated water does not guarantee consistency in the individual contributions of evaporation and blowdown, as illustrated in Fig. 15.

Fig. 15 compares the monthly water consumption against values estimated by a performance model for the year 2024. Both data sets exhibit a predictable seasonal trend, with consumption peaking during the summer months in correlation with higher solar irradiance and cooling demand. However, the graph reveals significant discrepancies between the actual and modeled data. Most notably, registered consumption substantially exceeded predictions in March, August, and September, while a pronounced drop in consumption occurred in June. A quantitative analysis of the model's error, measured by the Mean Absolute Percentage Error (MAPE), reveals the specific sources of inaccuracy. The most relevant finding is the exceptionally high average MAPE of 33.29% for blowdown, which provides quantitative evidence that the plant's cycles of concentration were not constant as assumed by the model but were managed dynamically. Furthermore, the significant average MAPE of 16.40% for evaporation and drift confirms that the plant's actual thermal load and operating hours deviated from the simulation, consistent with periods of outage or reduced generation. Given that evaporative loss is the single largest component of water consumption highlights the need for a more precise calculation model. Such a model must move beyond steady-state assumptions to incorporate the dynamic, hourly thermal load rejected by the power block, thereby accurately reflecting part-load operation, shutdowns, and start-ups. Furthermore, it should be based on high-resolution meteorological data and a more sophisticated cooling tower performance model that can predict off-design behavior.

As a conclusion to this section, the SAM model has been validated using experimental data on both electricity production and

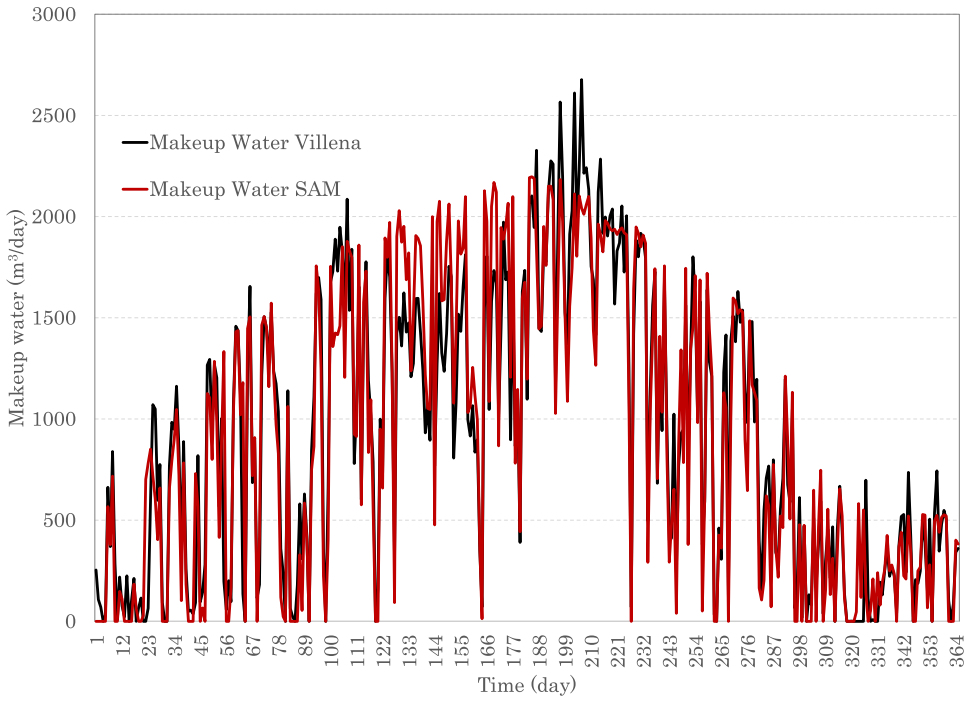

Fig. 14. SAM and real makeup water consumption. Daily data.

Fig. 15. SAM and real water consumption. Monthly data.

water consumption, obtained from the Villena solar plant, allowing for the assessment of its precision and reliability. The energy parameters analyzed, which encompass energy generation and capacity factor at annual, monthly, daily, and hourly scales, have demonstrated good concordance with actual measurements, thus confirming the model's suitability for simulation purposes. Concerning evaporated water, it is concluded that the hourly resolution is not appropriate for balance calculations, as it results in inconsistent scenarios. However, model tuning allows for its validation in terms of composition of water, although the apparent independence of evaporated water from environmental conditions warrants further investigation in future studies.

3. Cooling systems under investigation

Wet cooling systems, included by default in SAM, consist of a shell-and-tube condenser that utilizes recirculated water from a cooling tower as its cold sink. Cooling tower thermal performance can be approached through various modeling methodologies, ranging from highly simplified to comprehensive mechanistic models. On one end

of the spectrum are simplistic approaches, such as those typically integrated into SAM, which often approximate performance by fixing temperature differences (e.g., approach and range) with respect to the ambient wet-bulb temperature. These models offer a practical and computationally efficient means for system-level simulations. Conversely, more detailed and rigorous models delve into fundamental mass and energy balances between the interacting air and water streams within the cooling tower. An exemplary approach in this category is the model proposed by [25], which meticulously accounts for heat and mass transfer phenomena, providing a more granular and accurate prediction of tower performance under varying conditions. For this work, we have adopted SAM's inherent modeling approach for cooling tower thermal performance. Incorporating a more complex, physics-based model, such as Poppe's, is reserved for future research to further refine the predictive capabilities. Consequently, the key equations employed within SAM for the cooling tower model are:

$$T_{cond} = T_{wb} + \Delta T_{app} + \Delta T_{cw} + \Delta T_{out} \tag{6}$$

$$\Delta T_{app} = T_{cw,out} - T_{wb} \tag{7}$$

$$\Delta T_{cw} = T_{cw,in} - T_{cw,out} \tag{8}$$

The heat rejected ($Q_{rej,wet}$) by the cooling tower is given by:

$$Q_{rej,wet} = \dot{m}_{cw} \cdot c_p \cdot \Delta T_{cw} \tag{9}$$

A lower approach temperature indicates a more efficient tower, leading to a lower T_{cond} and thus a better vacuum at the turbine exhaust, enhancing power output.

$$Q_{rej,wet} = P_{\text{cycle}} \left(\frac{1}{\eta_{\text{T}}} - 1 \right) \tag{10}$$

The power cycle model is fundamentally based on a design-point performance, which is then adjusted hourly based on actual operating conditions. The user defines a design-point efficiency at full load under specific ambient conditions (either wet-bulb or dry-bulb temperature, depending on the cooling system), representing the maximum achievable cycle efficiency. For off-design scenarios, SAM applies correction curves or lookup tables to adjust this efficiency. This part-load performance is a function of the thermal load from the solar field or storage, the inlet temperature of the heat transfer fluid (HTF), and critically, the ambient temperature, which directly impacts the condenser pressure and overall cycle efficiency.

Furthermore, the power cycle model is intrinsically coupled with the selected cooling system (wet, dry, or hybrid). The ambient temperature dictates the condenser pressure and, consequently, the net work output of the turbine; higher ambient temperatures reduce cycle efficiency, an effect that SAM quantifies using performance correction functions. The model also calculates the parasitic energy consumption of the cooling system components, such as pumps and fans, and subtracts this load from the gross electric output to determine the net power delivered to the grid.

$$\eta_{\text{T}} = f(T_{cond}) \tag{11}$$

Air cooled condensers (ACC) are the inherently selected dry cooling technology within SAM. ACCs transfer heat from the condensing steam directly to the ambient air, making the ambient dry-bulb temperature (T_{db}) the primary environmental factor influencing performance. The Initial Temperature Difference (ITD) is a critical design and operational parameter, defined as the difference between the saturation temperature of the steam entering the condenser (T_{cond}) and the ambient dry-bulb temperature:

$$\text{ITD} = T_{cond} - T_{db} \tag{12}$$

A smaller ITD generally indicates a more efficient ACC design, allowing for lower condenser pressures at a given ambient temperature. The heat rejected ($Q_{rej,dry}$) by an ACC is calculated based on fundamental heat transfer principles:

$$Q_{rej,dry} = U \cdot A \cdot \text{LMTD} \tag{13}$$

Here, U represents the overall heat transfer coefficient, A is the total heat transfer area of the condenser, and LMTD is the Log Mean Temperature Difference between the condensing steam and the cooling air. The LMTD inherently accounts for the temperature change of the air as it passes through the condenser.

Parallel combined cooling systems are a feature within the System Advisor Model (SAM), complementing the established wet and dry cooling approaches. This configuration involves arranging an undersized wet-cooling system in parallel with a standard or slightly undersized air-cooled condenser (ACC). As established by [26], the parallel hybrid cooling architecture represents a noteworthy technological approach, as it concurrently limits the water requirements of the power plant and lessens the performance losses associated with dry heat rejection systems.

The fundamental premise underlying this technology is that air cooling provides adequate heat rejection capacity for the majority of a plant's operational duration. However, dry cooling system performance is most severely compromised during summer afternoon hours, periods when both ambient temperatures and electricity sales revenue typically reach their highest points. During these peak summer periods, the elevated temperature rise of the cooling airstream across the ACC is substantial. Integrating a wet-cooling system in parallel allows for a shared heat rejection load, which consequently diminishes this temperature rise and enhances the overall thermodynamic efficiency of the power cycle.

Distinct from exclusively wet-cooling systems, whose performance is governed by the wet-bulb temperature, the combined system's performance is driven by the dry-bulb temperature. Due to the interconnection of the wet and dry cooling components, the condensing steam pressure is uniform across both subsystems. If, theoretically, the steam pressure (and its corresponding temperature) were to fall below the dry-bulb temperature, thermal energy transfer from the ambient air into the ACC would occur, thereby negating the purpose of the dry-cooling system. Therefore, the thermodynamic performance of a combined system is bounded, falling between the lower limit of a non-ideal dry-cooling system and the upper limit of an ideal dry-cooling system (defined as an ACC achieving a steam temperature equivalent to the ambient dry-bulb temperature).

For each timestep during the simulation, the heat rejection load handled by the wet cooling system is calculated as a user-specified fraction of the total cooling demand. Consequently, the total heat rejection load ($\dot{Q}_{rej}$) is distributed such that the heat rejected by the air-cooled (dry) system ($\dot{Q}_{rej,air}$) and the wet-cooled system ($\dot{Q}_{rej,wc}$) are given by the following equations, where f_{wc} represents the fraction of total cooling handled by the wet system for the current timestep:

$$\dot{Q}_{rej,air} = (1 - f_{wc})\dot{Q}_{rej} \tag{14}$$

$$\dot{Q}_{rej,wc} = f_{wc}\dot{Q}_{rej} \tag{15}$$

The total heat rejected ($Q_{rej,total}$) by a parallel combined system is the sum of the heat rejected by each component:

$$Q_{rej,total} = Q_{rej,wet} + Q_{rej,dry} \tag{16}$$

It is important to note that the valid range for the wet cooling fraction is $0 \leq f_{wc} < 1$, indicating that the dry cooling system always handles at least some portion of the load or can be the sole cooling method when $f_{wc} = 0$. This flexible dispatch strategy allows for dynamic optimization of water consumption and power output based on prevailing conditions and operational objectives.

The performance equations for the hybrid configuration are nearly identical to those for individual technologies, with the primary difference being the heat rejection load each subsystem accommodates

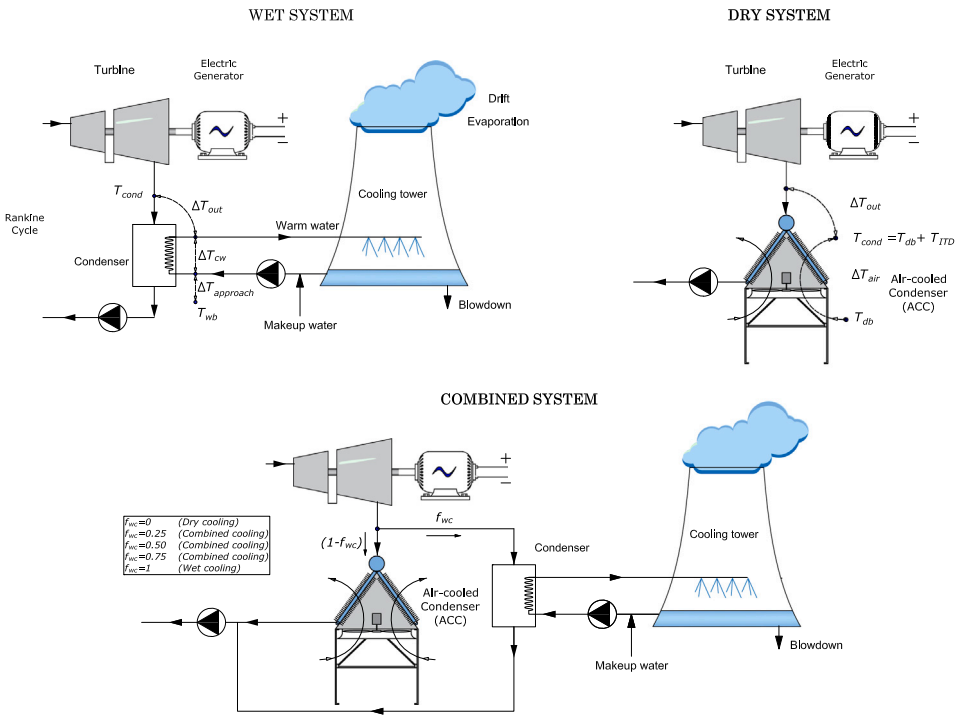

Fig. 16. Cooling systems compared: Wet, dry, and combined systems.

relative to its design point. The ACC is typically sized to handle the full heat rejection load throughout the year, while the wet-cooling system is sized to match its largest required heat rejection load annually. SAM calculates the condenser pressure for the hybrid system by first determining the performance of each cooling system individually, then taking the maximum of the two condenser pressures as the actual achieved pressure:

$$P_c = \max(P_{c,WC}, P_{c,ACC}) \tag{17}$$

where $P_{c,WC}$ is the condenser pressure if only the wet cooling system were operating, and $P_{c,ACC}$ is the condenser pressure if only the Air-Cooled Condenser were operating.

In SAM, parasitic power consumption for cooling systems, crucial for determining net electricity, is rigorously modeled. For wet cooling towers, loads primarily involve fans and circulating water pumps. These are calculated based on component design and operating conditions, often using polynomial functions correlating power to air and water flow rates, respectively. For Air-Cooled Condensers (ACCs), large fans constitute the dominant parasitic load, significantly higher due to the massive air volumes required. SAM simulates this based on ACC design and ambient conditions, noting its sensitivity to temperature. These calculated parasitic losses are then subtracted from gross generation, providing the true net power output. For a comprehensive review of the equations detailed within this section, including their derivation and specific parameters, refer to the SAM Technical Reference Manual, [27] (see Fig. 16).

4. Results and discussion

4.1. Results

Once the model has been described, validated using real operating data from the plant, and the cooling options provided by SAM for the CSP plant have been outlined, this section presents the results for the conventional condensation solutions — wet and dry — as well as for three combined parallel configurations with $f_{wc} = 0.25, 0.50$, and 0.75.

Table 2 displays the set of results linked to the five simulations conducted for the different cooling configurations. The data illustrates the critical trade-off between net electricity generation and water consumption in CSP plants across various cooling technologies. Wet cooling, while delivering the highest Annual AC Energy (79.1 GWh), incurs the most significant water demand (277,443 m^3), establishing it as the baseline for both performance and water intensity. Conversely, dry cooling substantially reduces water usage by 91.5% (23,566 m^3), yet this comes at a notable cost to energy production, exhibiting an 11.5% reduction in Annual AC Energy compared to its wet-cooled counterpart. For the parallel combined cooling systems, net electricity generation experiences negligible impact, with reductions consistently below 1%. Simultaneously, these configurations yield water consumption savings of 24.2%, 46.6%, and 69.1% for the respective cases examined.

In line with the annual data, the analysis of monthly data reveals that throughout the year, the electrical production of the combined system (especially the 50% wet and 25% wet configurations) remains very close to that of the 100% wet system, with differences consistently below 1% in most months, see Fig. 17. This indicates the feasibility of maintaining similar generation levels with a significant reduction in water consumption. In contrast, the 100% dry system significantly reduces production, particularly during the warmer months (e.g., July and August), with declines of up to 7%–9% compared to the wet system. A noteworthy observation is that during the months of March, April, May, and June, the production of some of the combined systems surpasses that of the wet system. This phenomenon occurs because in these months the condensation temperature is lower with the parallel system, leading to a more efficient Rankine cycle, and thus enabling greater electricity generation. Specifically, in March, the combined systems 50% wet and 25% wet show an increase in production of 0.25% and 0.04%, respectively. In April and May, the combined system 50% produces 0.17% and 0.1% more, respectively. The 75% wet combined system also slightly outperforms with 0.02% and 0.06% increases in May and June, respectively. Consequently, the improved performance of the hybrid system over the wet-cooled configuration during certain months of the year implies that, once the system is sized, regulating the operational fraction between the air-cooled condenser (ACC) and the wet-cooling section is critical for maximizing electrical power output while minimizing water consumption.

Table 2
Performance metrics under different wet conditions.

Metric	Wet cooling	0.75 WET	0.5 WET	0.25 WET	Dry cooling
Annual AC energy in year 1 (kWh-e)	79,088,952.0	78,356,408.0	78,515,448.0	78,297,000.0	69,988,448.0
Capacity factor (%)	18.0586	17.8914	17.9277	17.8778	15.9807
Power cycle gross electrical output (kWh-e)	94,694,008.0	97,417,640.0	97,111,808.0	96,657,992.0	88,421,024.0
First Year kWh/kW	1582.0	1567.3	1570.0	1566.1	1399.9
Gross-to-Net conversion (%)	83.5206	80.4335	80.8506	81.0042	79.1536
Annual water usage (m^3)	277,443.0	210,323.0	148,097.0	85,689.6	23,566.2
Ratio water/energy (m^3/MWh)	3.5	2.7	1.9	1.1	0.3
%Annual AC energy (%)	100.0	99.1	99.3	99.0	88.5
%Annual water usage (%)	100.0	75.8	53.4	30.9	8.5
%Annual AC energy reduction (%)	0.0	−0.9	−0.7	−1.0	−11.5
%Annual water usage savings (%)	0.0	24.2	46.6	69.1	91.5

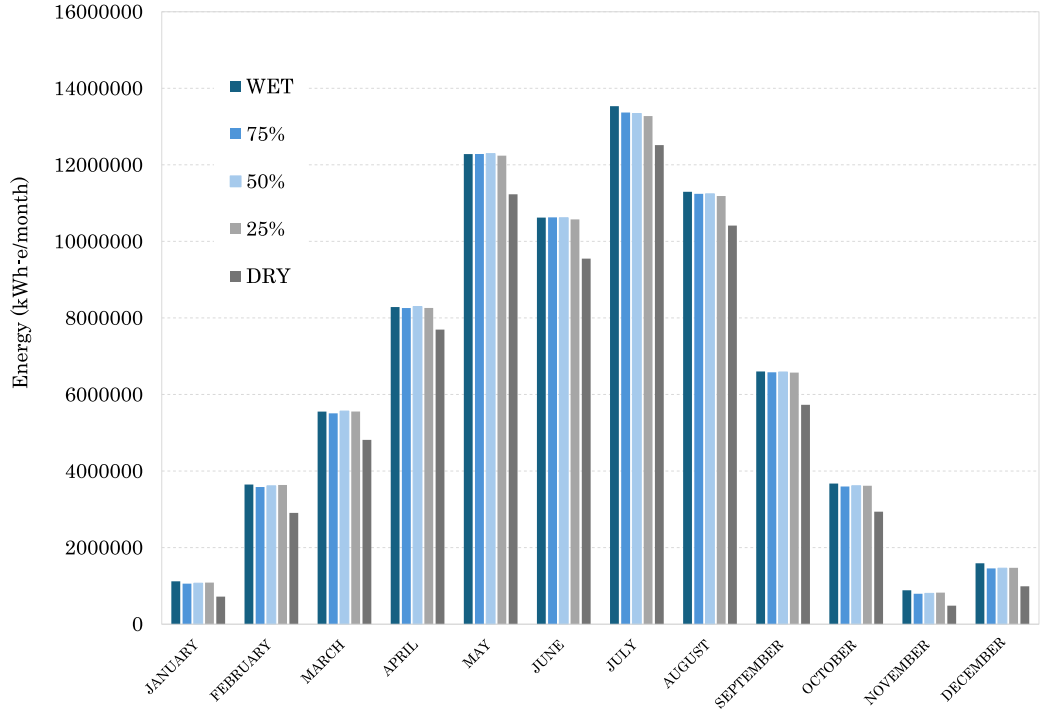

Fig. 17. Comparison of monthly energy generation for the analyzed cooling systems.

Regarding water consumption, the wet system exhibits very high values throughout the year, with peak consumption exceeding 39,000 m^3/month during the months of maximum solar radiation (May–August), see Fig. 18. In contrast, combined configurations achieve progressive reductions in water usage. This behavior demonstrates that it is possible to achieve substantial water savings without significantly compromising electrical production, especially in intermediate configurations. The advantage of the combined system is particularly notable during months of higher thermal demand, when the dry system experiences greater performance degradation. In these periods, the combined system allows for operational flexibility: prioritizing the use of the wet system during critical moments to ensure production, while under more favorable conditions (winter and spring), a larger dry fraction can be operated, thereby minimizing water consumption. The analyzed data reflect that the implementation of a combined condensation system allows for an optimal compromise between energy efficiency and environmental sustainability. The 50% or 25% wet configuration appears to be the most advisable for hot and dry climates, where water resources are limited, but maintaining high and stable energy production throughout the year is desired.

4.2. Economic evaluation

With the potential advantages of incorporating a parallel cooling system established, the selection of the most appropriate option from the analyzed alternatives becomes paramount. This requires an economic assessment that weighs the benefits of reducing water consumption against the power generation penalty and the incremental capital expenditure associated with each proposed solution.

Forecasting long-term electricity and water prices is an inherently challenging task, a difficulty that has been significantly amplified by recent events in the Spanish energy market. A critical grid failure in April 2025 led to widespread blackouts, forcing a strategic re-evaluation by the national grid operator. This situation has prompted a regulatory shift to prioritize grid stability, resulting in a renewed reliance on dispatchable fossil-fuel technologies. Such unpredictable events and the subsequent reactive policy changes underscore the profound volatility of the energy market, making any economic analysis based on fixed price projections unreliable.

The water supply for the Villena Solar Thermal power plant is notably diverse, reflecting a water management strategy adapted to regional constraints. The facility utilizes a portfolio of sources, including captured rainwater, irrigation water, and the municipal supply

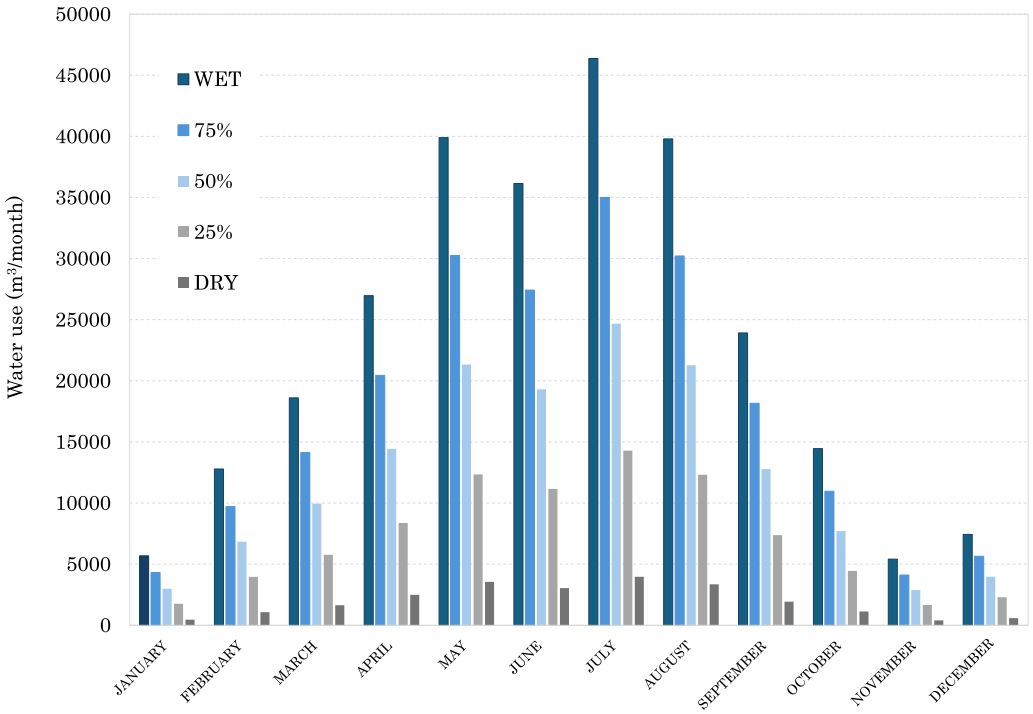

Fig. 18. Comparison of monthly water consumption for the analyzed cooling systems.

network. Uniquely, the plant also draws upon treated effluent from the wastewater reclamation facility of an adjacent prison (see Fig. 1), representing a noteworthy example of circular economy principles and integrated resource management in a water-scarce environment. This diversity of water origins, and therefore their associated costs, complicates the determination of a single blended water price.

This economic uncertainty necessitates a parametric approach to assessing the viability of the proposed retrofits. The analysis, therefore, considers a spectrum of future scenarios, with electricity prices ranging from 0.05 to 0.3 €/kWh$_e$ and water costs from of 1.25 to 5 €/m^3.

This retrofitting analysis is contextualized by the plant's operational timeline, as the study is conducted at the midpoint of its nominal 25-year lifespan. Consequently, a critical criterion for the financial viability of any proposed solution is a payback period of less than the remaining 12 years of operation. While future operational extensions or license renewals for the plant could be considered, this 12-year threshold serves as a conservative benchmark for assessing the investment's feasibility within the currently projected operational framework.

Taking into account the operating costs, Fig. 19 can be obtained. The most advantageous situation is obviously obtained when the cost of water is at its highest and the cost of electricity is at its lowest. It becomes evident that in economic terms the water savings of the dry system do not compensate for the large loss of production. Analyzing the systems, the most beneficial is the 25% wet combined system, followed by the 50% wet system, and in comparison, the benefit of the 75% wet system is low. It can also be observed that the benefit across the different ranges increases as it approaches between point 20 and 30 (25% wet combined system), highlighted, and how it progressively decreases to negative values at point 0 (dry system).

To perform an economic feasibility study, it is proposed to analyze the simple payback period of the different solutions. For this, it is necessary to estimate the cost of the ACC. To determine the estimated cost of the air-cooled condenser, the energy analysis of the system is used as a starting point. Considering that the thermal power plant has a net electrical output of 50 MW and an overall efficiency of 39.71%, the total thermal energy required can be calculated based on Eq. (10). In this case, this energy is approximately 125.91 MW. Of this total energy, the part that is not converted into electricity must be dissipated into the environment through the cooling system. This waste heat, or rejected heat, amounts to about 75.91 MW.

Subsequently, an analysis is performed to determine the thermal load distribution among the constituent components of the combined cooling system, specifically differentiating between the evaporative cooling tower (wet mode) and the air-cooled condenser (dry mode). Three operation scenarios are considered, in which the percentage of heat dissipated by the air-cooled condenser varies. In the first case, where the system operates 75% in wet mode, the air-cooled condenser assumes 25% of the total thermal load, which is equivalent to approximately 18.98 MW$_t$.

In the second case, with an equal distribution of 50% between both systems, the air-cooled condenser dissipates approximately 37.96 MW$_t$. In the third scenario, where the use of the wet system is reduced to 25%, the air-cooled condenser is responsible for 75% of the heat, that is, 56.93 MW$_t$. With these values, the cost of the air-cooled condenser is estimated based on different unit prices per installed thermal kilowatt. Three levels of unit cost have been considered: 0.1 €/kW$_t$, 0.2 €/kW$_t$ and 0.3 €/kW$_t$. These ranges allow for potential variations in actual market prices, as well as different qualities or technologies of the equipment. Based on thermal requirements and investment costs range, an investment bracket is established, ranging from 1 897 821 € for the case of $f_{cw} = 0.75$ and 0.1 €/kW$_t$ up to 17 080 395 € for the case of $f_{cw} = 0.25$ and 0.3 €/kW$_t$.

Fig. 20 illustrates how the most favorable case is achieved when the water price is high and the electricity price is low. Specifically, the optimal scenario occurs with a water price of 5 €/m^3, an electricity price of 0.05 €/kW$_e$, and an air-cooled condenser that dissipates 50% of the waste heat (50% wet mode). Under these conditions, and with an air-cooled condenser cost of 0.1 €/kW$_t$, the investment payback period is approximately 6.14 years, which is considered a reasonably short timeframe for industrial installations of this type. The combined system with 50% participation from the wet system proves to be the most favorable. The 25% wet system, although having slightly higher payback periods, still remains within reasonable margins. Furthermore, the 75% wet system presents competitive values, but with a higher average payback period.

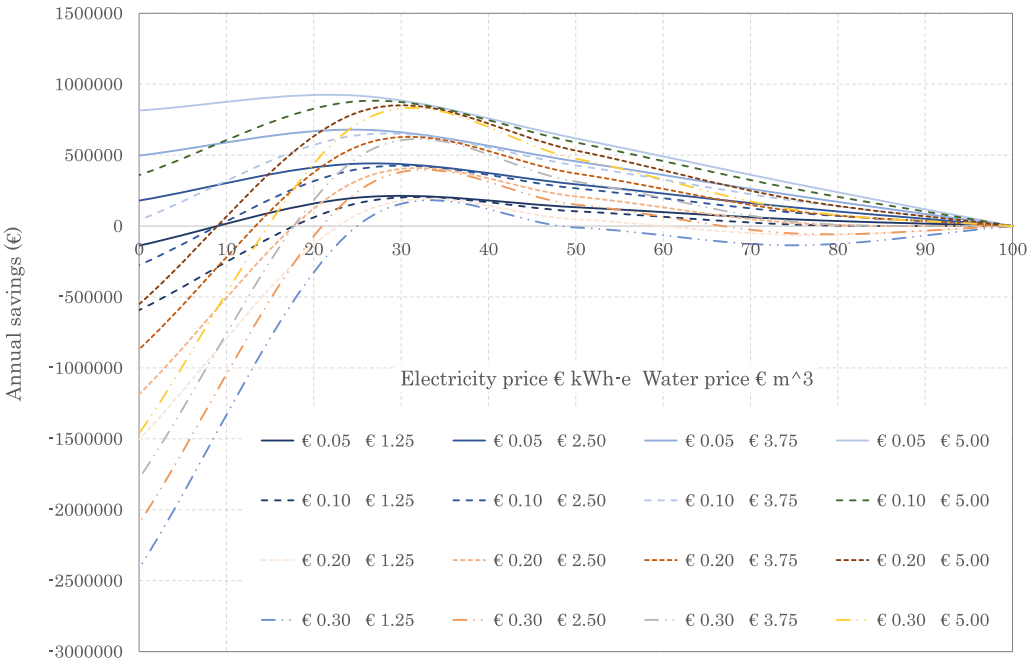

Fig. 19. Annual savings for different wet cooling system percentages.

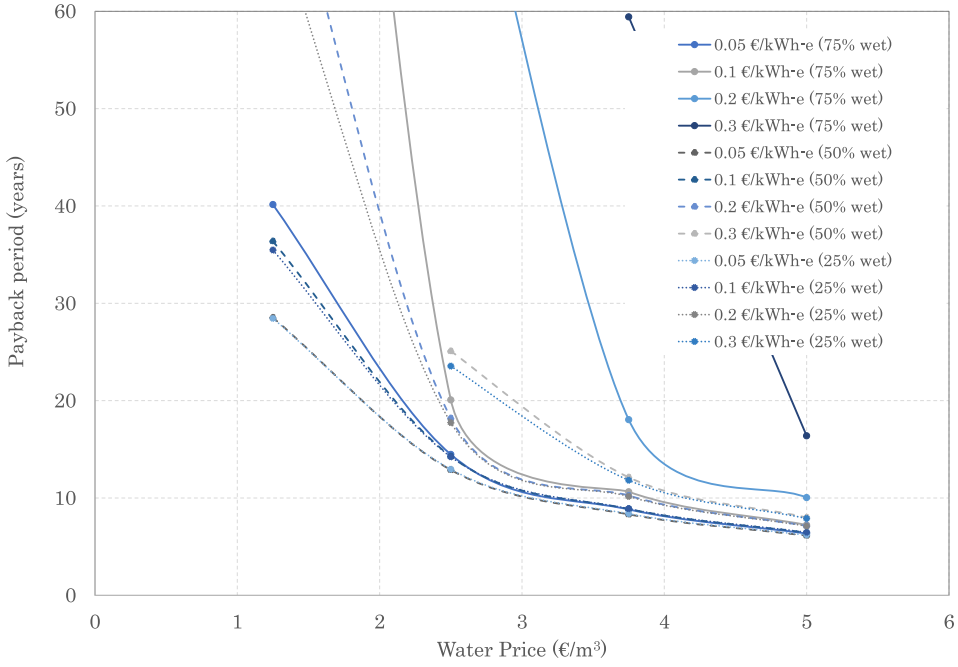

Fig. 20. Payback periods for different wet cooling system percentages with an ACC cost of 0.1 €/kW$_t$.

Conversely, when water prices are low and electricity costs are high, the system tends to become economically unfeasible. For instance, with a water price of 1.25 €/m^3 and an electricity cost of 0.3 €/kW$_e$, annual profits can become negative. This is evidenced in scenarios where the return on investment significantly exceeds 20 years or is not achieved at all, rendering such configurations economically unadvisable. At an air-cooled condenser cost of 0.3 €/kW$_t$, representing the highest cost per installed thermal unit, the observed trend is significantly accentuated. The 75% wet system becomes distinctly unfeasible, exhibiting payback periods exceeding 100 years, thereby precluding it as a practical option. Conversely, the 50% wet combined system, despite being affected by increased costs, continues to offer reasonable payback periods within a range of 18 to 26 years. The 25% wet system, while viable in specific contexts, only achieves competitive payback times in scenarios characterized by elevated water prices.

Following the comprehensive techno-economic analysis, it is concluded that a hybrid cooling system, comprising a 50% evaporative cooling tower and a 50% air-cooled condenser, represents the most suitable configuration for industrial applications aiming to optimize the balance between sustainability, initial capital expenditure, and economic viability. This specific arrangement facilitates a substantial reduction in water consumption without incurring prohibitive costs, while maintaining a reasonable return on investment (ROI) period, even under conditions of elevated energy costs. Therefore, its implementation is advocated as a versatile, efficient, and scalable solution. These findings align with a recent techno-economic review of CSP,

which evaluated the technology's cost competitiveness and deployment potential, [28].

5. Conclusions and future perspectives

5.1. Conclusions

This study investigated the technical and economic feasibility of retrofitting a Concentrated Solar Power (CSP) plant with a combined cooling system aimed at reducing water consumption without significantly compromising power generation. Using the System Advisor Model (SAM), the Enerstar-Villena CSP plant was accurately modeled and validated with real operational data from the full year 2024, ensuring high reliability of the simulation outputs.

- **Model validation:** The SAM model demonstrated excellent agreement with real plant data in terms of electricity production and water consumption, achieving a Mean Absolute Percentage Error (MAPE) below 1.1% for annual energy output and 0.4% for annual water consumption.
- **SAM Limitations:**: The water evaporation calculation is oversimplified, relying solely on the latent heat of vaporization; more sophisticated methods like the Poppe model are necessary for accuracy, in line with the work of [29]. Additionally, SAM cannot model key retrofitting options, such as air-coolers in parallel with cooling towers or adiabatic pre-cooling systems.
- **Cooling strategies:** Among the five analyzed cooling configurations — wet, dry, and three combined systems — combined cooling systems exhibited strong potential to balance water savings and energy efficiency.
- **Optimal configuration:** The configuration with 50% wet and 50% dry cooling achieved the most favorable balance, reducing water consumption by 46.6% with less than 1% loss in net electricity generation.
- **Energy performance:** Some combined configurations even showed slight improvements in energy output during spring months, driven by more favorable condensation temperatures in the hybrid setup.
- **Economic viability:** The 50% wet/50% dry system demonstrated the best trade-off between investment cost and operational savings, with a payback period as low as 6.1 years under favorable economic assumptions.

Therefore, it is concluded that retrofitting existing CSP plants with a parallel combined cooling system — particularly with a balanced wet/dry load share — represents a highly effective strategy for reducing water usage while maintaining high operational efficiency. This approach also enhances plant flexibility and resilience in regions facing increasing water scarcity.

5.2. Future perspectives

Building on the results of this work, several future research directions are proposed:

- **Engineering design of the air-cooled condenser (ACC):** A more detailed engineering study is recommended, focusing on the sizing of the ACC and the selection of fans. Notably, a suitable and sufficient area has already been identified in the southwest section of the Balance of Plant (BOP) as the optimal location to install the additional ACC.
- **Alternative heat rejection configurations:** Future studies should explore new cooling configurations beyond those analyzed in this work. A priority will be the evaluation of connecting an air-cooled heat exchanger (ACHE) either in series or in parallel with the existing cooling tower. In particular, a configuration that connects the ACHE directly to the hot water pipe exiting the condenser is considered, as this approach is technically simpler and more straightforward to implement.
- **Hybridization of dry cooling units:** It is advisable to assess the potential for hybridizing the ACC or the ACHE by incorporating air pre-cooling techniques. This could involve the use of evaporative pads or water atomization systems at the air inlet to enhance cooling performance, especially during peak thermal loads.
- **Improved modeling of evaporative losses:** A refinement of the evaporated water calculation in the cooling tower is also proposed. The use of a more accurate physical model, such as the Poppe model, could more realistically capture the effect of ambient conditions on water consumption. This would address the limitations of the default simplified approach currently used by SAM and improve water management strategies under varying climate scenarios.
- **Thermal energy storage and hybridization with photovoltaic (PV):** Another alternative to be considered during the retrofitting phase of the plant is the potential incorporation of thermal energy storage and even hybridization with photovoltaic (PV) systems, in order to better align electricity production with grid demand.

CRediT authorship contribution statement

M. Lucas: Writing – original draft, Validation, Methodology, Funding acquisition, Formal analysis, Conceptualization. **J. Catalán:** Writing – review & editing, Resources, Data curation, Conceptualization.

Declaration of Generative AI and AI-assisted technologies in the writing process

During the preparation of this work, the author used ChatGPT (OpenAI) and Gemini (Google) to assist in drafting and editing parts of the manuscript, particularly in refining the English language. After using these tools, the author reviewed and edited the content as needed and takes full responsibility for the content of the published article.

Declaration of competing interest

The authors declare that they have no known competing financial interests or personal relationships that could have appeared to influence the work reported in this paper.

Acknowledgments

This publication is part of the R&D project CIAEST/2022/82, "Research on Innovative Heat Dissipation Systems for Water Savings at the Enerstar Villena Concentrated Solar Power Plant" funded by Conselleria de Innovación, Universidades, Ciencia y Sociedad Digital (GVA). The authors also wish to acknowledge the collaboration of Mechanical Engineering student R. M. Portales in the SAM simulations.

Data availability

Data will be made available on request.

References

[1] International Energy Agency (IEA), Net zero by 2050: A roadmap for the global energy sector, 2021, URL: https://www.iea.org/reports/net-zero-by-2050.
[2] European Commission, REPowerEU Plan: A plan to rapidly reduce dependence on Russian fossil fuels and fast forward the green transition, 2022, URL: https://eur-lex.europa.eu/legal-content/EN/TXT/?uri=CELEX%3A52022DC0230.
[3] International Renewable Energy Agency (IRENA), Renewable energy technologies: Innovation outlook for concentrated solar power, 2022, URL: https://www.irena.org/publications/2022/Sep/Innovation-Outlook-Concentrated-Solar-Power.
[4] EPRI, Comparison of Alternate Cooling Technologies for California Power Plants: Economic, Environmental, and Other Trade-offs, Technical Report, 2002, URL: https://www.epri.com/research/products/000000000001005358.
[5] A. Cooperman, J. Dieckmann, J. Brodrick, Power plant water use, ASHRAE J. 54 (2012) 65–68.

[6] A. Poullikkas, I. Hadjipaschalis, G. Kourtis, A comparative overview of wet and dry cooling systems for rankine cycle based CSP plants, Trends Heat Mass Transf. 13 (2013) 27–50.
[7] A.M. Blanco-Marigorta, M. Victoria Sanchez-Henríquez, J.A. Peña-Quintana, Exergetic comparison of two different cooling technologies for the power cycle of a thermal power plant, Energy 36 (4) (2011) 1966–1972, http://dx.doi.org/10.1016/j.energy.2010.09.033, URL: https://www.sciencedirect.com/science/article/pii/S0360544210005128, 5th Dubrovnik Conference on Sustainable Development of Energy, Water & Environment Systems.
[8] R. Patnode, Detailed heat and energy transfer analysis for a 30 MWe CSP plant, 2006, Developed and solved a model using EES and TRNSYS software. Examined the impact of replacing the wet cooling system with an air-cooled condenser. Results showed a considerable reduction in energy production, estimated at 1.3 MWe.
[9] A.H. Graaff, Performance Evaluation of a Hybrid (Dry / Wet) Cooling system (Thesis), Stellenbosch University, Stellenbosch, South Africa, 2017.
[10] C. Cutillas, J. Ruiz, F. Asfand, K. Patchigolla, M. Lucas, Energetic, exergetic and environmental (3E) analyses of different cooling technologies (wet, dry and hybrid) in a CSP thermal power plant, Case Stud. Therm. Eng. 28 (2021) 101548.
[11] L. Redelinghuys, M. Tshamala, T. Hans, Performance of an adiabatic pre-cooling system for concentrating solar power plants in arid areas, Appl. Therm. Eng. 231 (2023) 120819, http://dx.doi.org/10.1016/j.applthermaleng.2023.120819, URL: https://www.sciencedirect.com/science/article/pii/S1359431123008487.
[12] C. Turchi, M. Wagner, C. Kutscher, Water Use in Parabolic Trough Power Plants: Summary Results from WorleyParsons' Analyses, Technical Report NREL/TP-5500-49468, National Renewable Energy Laboratory, Golden, 2010.
[13] M. Palmero-González, E. Batuecas, M. Fernandez-Torrijos, C. Marugan-Cruz, Environmental comparison of dry and hybrid condensing systems in concentrating solar power tower plants, Energy Convers. Manage. 340 (2025) 119978, http://dx.doi.org/10.1016/j.enconman.2025.119978, URL: https://www.sciencedirect.com/science/article/pii/S0196890425005023.
[14] F. Asfand, P. Palenzuela, L. Roca, A. Caron, C.-A. Lemarié, J. Gillard, P. Turner, K. Patchigolla, Thermodynamic performance and water consumption of hybrid cooling system configurations for concentrated solar power plants, Sustainability 12 (11) (2020) http://dx.doi.org/10.3390/su12114739.
[15] P. Palenzuela, L. Roca, F. Asfand, K. Patchigolla, Experimental assessment of a pilot scale hybrid cooling system for water consumption reduction in CSP plants, Energy 242 (2022) 122948, http://dx.doi.org/10.1016/j.energy.2021.122948, URL: https://www.sciencedirect.com/science/article/pii/S0360544221031972.
[16] National Renewable Energy Laboratory, Solarpaces, 2025, n.d. https://solarpaces.nrel.gov/. (Accessed 15 April 2025).
[17] S. Bogart, SankeyMATIC, 2025, from https://sankeymatic.com/. (Accessed 15 April 2025).
[18] National Renewable Energy Laboratory (NREL), CSP validation, 2025, from https://sam.nrel.gov/concentrating-solar-power/csp-validation.html. (Accessed 15 April 2025).
[19] A. Boretti, J. Nayfeh, W. Al-Kouz, Validation of SAM modeling of concentrated solar power plants, Energies 13 (10) (2020) 2549, http://dx.doi.org/10.3390/en13102549.
[20] W. Al-Kouz, A. Almuhtady, N. Abu-Libdeh, J. Nayfeh, A. Boretti, A 140 MW solar thermal plant in Jordan, Processes 8 (6) (2020) http://dx.doi.org/10.3390/pr8060668, URL: https://www.mdpi.com/2227-9717/8/6/668.
[21] E.K. Ezeanya, System Advisor Model (SAM) Simulation Modeling of a Concentrating Solar Thermal Power Plant with Comparison to Actual Performance Data (Master's thesis), University of Louisiana at Lafayette, 2017.
[22] Real decreto 487/2022, de 21 de junio, por el que se establecen los criterios higiénico-sanitarios para la prevención y control de la legionelosis, 2022, URL: https://www.boe.es/buscar/act.php?id=BOE-A-2022-10297, Boletín Oficial del Estado, núm. 148, de 22 de junio de 2022. Entrada en vigor: 2 de enero de 2023.
[23] M. Poppe, H. Rögener, Berechnung von rückkühlwerken, VDI Wärmeatlas (1991) Mi 1.
[24] Instituto para la Diversificación y Ahorro de la Energía (IDAE), Guía Técnica de Torres de Refrigeración, Instituto para la Diversificación y Ahorro de la Energía, Madrid, Spain, 2007.
[25] J.C. Kloppers, D.G. Kröger, Cooling tower performance evaluation: Merkel, Poppe, and e-NTU methods of analysis, J. Eng. Gas Turbines Power 127 (1) (2005) 1–7, http://dx.doi.org/10.1115/1.1787504.
[26] M.J. Wagner, C. Kutscher, The impact of hybrid wet/dry cooling on concentrating solar power plant performance, in: Proceedings of the 4th International Conference on Energy Sustainability, Vol. ES2010-90442, Phoenix, Arizona, USA, 2010.
[27] M.J. Wagner, P. Gilman, Technical Manual for the SAM Physical Trough Model, Technical Report NREL/TP-5500-51825, National Renewable Energy Laboratory (NREL), Golden, CO (United States), 2011, http://dx.doi.org/10.2172/1018925.
[28] M.I. Khan, R. Gutiérrez-Alvarez, F. Asfand, Y. Bicer, S. Sgouridis, S.G. Al-Ghamdi, H. Jouhara, M. Asif, T.A. Kurniawan, M. Abid, A. Pesyridis, M. Farooq, The economics of concentrating solar power (CSP): Assessing cost competitiveness and deployment potential, Renew. Sustain. Energy Rev. 200 (2024) 114551, http://dx.doi.org/10.1016/j.rser.2024.114551, URL: https://www.sciencedirect.com/science/article/pii/S1364032124002740.
[29] P. Navarro, J. Serrano, L. Roca, P. Palenzuela, M. Lucas, J. Ruiz, A comparative study on predicting wet cooling tower performance in combined cooling systems for heat rejection in CSP plants, Appl. Therm. Eng. 253 (2024) 123718, http://dx.doi.org/10.1016/j.applthermaleng.2024.123718, URL: https://www.sciencedirect.com/science/article/pii/S1359431124013863.